Journal of Materials Chemistry A

RSC Publishing

PAPER

View Article Online
View Journal | View Issue

Epoxidized natural rubber–magnetite nanocomposites for oil spill recovery†

Cite this: *J. Mater. Chem. A*, 2013, **1**, 868

Swarnalatha Venkatanarasimhan and Dhamodharan Raghavachari*

New, eco-friendly nanocomposite materials have been synthesized from natural rubber (NR) and magnetite nanoparticles for the first time. The poor oil resistance of natural rubber is exploited for the removal of oil spills. Towards this purpose, mildly epoxidized natural rubber (ENR)–magnetite nanoparticle (MN) nanocomposites are prepared and the absorption of petrol (gasoline) is studied. The extent of epoxidation is controlled in such a manner that the NR does not lose its elasticity while retaining to a significant degree its oil absorbing property. Epoxidation also serves as a means for binding sufficient quantity of MNs so that the composite can be recovered using a magnetic field. ENR with 5 mol% of epoxidation served as the best absorbent among all the absorbents studied as it was stable in petrol even after many days of immersion. It is observed that the ENR–MN nanocomposite absorbs 7 g of petrol per gram without any mass loss. The material was reused for several cycles without much loss in the capacity. The petrol uptake of ENR–MN is greater than that of butyl rubber which is the most commercially used rubber for oil spill removal. Porous rubber was also synthesized for the first time as oil uptake is facilitated not only by the hydrophobicity but also by the capillary absorption. Porous ENR absorbed a relatively larger amount of oil and exhibited the highest stability in oil. All the sorbents have quite high absorption capacities to be applied practically with a very low water uptake and a few of the absorbents could be satisfactorily reused. The model studies promise their potential use in the environmental field.

Received 26th September 2012
Accepted 29th October 2012

DOI: 10.1039/c2ta00445c

www.rsc.org/MaterialsA

Introduction

Accidental discharge of crude oil into the sea during marine transportation is one of the most recurring pollutions occurring in the last few decades. Despite various precautions that have been taken, it is found to be impossible to avoid the involuntary oil spills completely. As the spilled oil is extremely detrimental to the marine ecosystem, it is indispensable to get rid of the oil slicks as soon as possible to safeguard the aquatic flora and fauna. Even after two decades, there are still various aftereffects due to *Exxon Valdez* oil spill.[1] The most extensively adopted techniques to clean up the oil spills are: (a) chemical treatment using dispersants or emulsion breakers; (b) *in situ* burning; (c) mechanical treatment using booms, skimmers, oil–water separators or sorbents and (d) bioremediation using microorganisms or biological agents.[2] Among these techniques, the usage of sorbents for oil spill treatment is considered to be beneficial as complete removal of oil is achieved. The fundamental criteria that have to be considered while choosing the oil sorbents are: (1) they should be hydrophobic and lipophilic either to adsorb or absorb the oil and (2) they should exhibit higher oil retention besides rapid and better oil pick up.[3] So far, a variety of sorbents have been used for oil spill removal. They can generally be classified as (a) natural materials such as milkweed, cotton, straw, vegetable fibers, sawdust, hydrophobic cotton fibers, non-woven wool, bagasse, nanocellulose aerogels;[3,4a–g] (b) synthetic materials such as polypropylene,[5a] polyurethane,[5b] phase selective organogelators[5c,d] and (c) inorganic materials such as fly ash, silica aerogel, exfoliated graphite, organophilic clays, and expanded perlite.[6a–e]

The most frequently used polymeric material for oil spill treatment is polypropylene as it has higher oil sorption capacity with lower uptake of water.[7] The major drawback with the polypropylene sorbent is that it is non-biodegradable and non-reusable. Natural rubber (NR) is a biodegradable and biocompatible polymer with specific mechanical properties such as high resilience, good tensile strength, and tear resistance. NR is a milky colloid produced by the tree *Hevea brasiliensis* with the chemical name of poly(*cis*-1,4-isoprene). The backbone of NR holds numerous non-collinear single covalent bonds about which rapid rotation is possible. These single bonds make the polymer extremely flexible, even at room temperature. However, NR has several disadvantages such as low oil resistance, poor wet skid resistance and poor weather resistance. To prevail over such limitations and fabricate

Department of Chemistry, Indian Institute of Technology Madras, Tamil Nadu 600 036, India. E-mail: damo@iitm.ac.in

† Electronic supplementary information (ESI) available. See DOI: 10.1039/c2ta00445c

materials with improved properties, chemical modifications of natural rubber such as epoxidation[8] and vulcanization are carried out.

Epoxidation produces rubber with randomly distributed epoxy groups along with the alkenic backbone and hence reduces the degree of unsaturation in natural rubber.[9] The introduction of oxirane groups into the natural rubber matrix results in elevation of the glass transition temperature, oil resistance and viscosity.[10] The resilience of natural rubber usually declines after the epoxidation reaction. Natural rubber was first epoxidized by Pummer and Burkhard in 1922. The epoxidation process using performic acid was later patented by Gelling[11] and this *in situ* epoxidation was found to be fairly effectual without even using any catalyst. In general, the epoxidation reaction using peracids is highly stereospecific and so the resultant epoxidized natural rubber (ENR) retains the stereoregularity of all the *cis*-1,4-configurations of the natural rubber. With higher percentage epoxidation, ENR turns harder due to the increasing gel content. Hence, a lower degree of epoxidation is advisable to preserve elasticity.

Polymer nanocomposites are a new class of materials in which one of the constituents is of nanometer dimension. They are better alternatives to their conventional microcomposite counterparts. The inclusion of nanosized fillers in the polymers significantly alters the properties of the corresponding polymers leading to the fabrication of innovative materials with potential applications. Magnetite is one of the most important iron oxides, which can be used as a nanofiller. Magnetite is considered to be the most magnetic of all the naturally occurring minerals on earth and magnetite nanoparticles (MNs) sized below 20 nm are superparamagnetic in nature.[12] Particularly, this extraordinary magnetic behaviour makes magnetite nanoparticles extremely useful in magnetic resonance imaging (MRI) contrast agents,[13a,b] magnetic storage devices,[13c] targeted drug delivery,[13d] and sensing applications.[13e] The superparamagnetism exhibited by magnetite nanoparticles can be exploited for the oil spill treatment by using them as inorganic fillers with an oleophilic polymer. After the oil absorption, the MN–polymer absorbents can be pulled off from the oil surface by using an external magnet. In 1973, Turbeville developed ferromagnetic sorbents for oil spill treatment by coating iron powder on polystyrene where the adsorbent necessary for the oil removal was 3 to 1 by volume of adsorbent to oil.[14]

In this work, the oil resistance of NR is enhanced by controlled epoxidation and magnetite nanoparticles are incorporated to acquire magnetically recoverable oil sorbents. MN is a Lewis acid and is expected to bond to the epoxidized natural rubber as well as natural rubber through acid–base (epoxide/double bond) interaction. Petrol is chosen as the model oil for the oil absorption studies. The ENR and ENR–magnetite nanocomposites function as a cost-effective and eco-friendly material (derived from renewable resources) for oil spill treatment, and thus could be preferred over the conventional non-biodegradable polymeric absorbents.

Experimental details

Materials used

Ferric chloride hexahydrate (Himedia, India), ferrous sulphate heptahydrate (RANKEM, India), 25% ammonium hydroxide (Merck, India), 98% formic acid (Merck, India), and 30% hydrogen peroxide (RANKEM, India) were all of analytical grade and used as received, without further purification. Natural rubber (NR) was obtained from Rubber Board, Kottayam, India. Butyl rubber was kindly donated by Hari Shankar Singhania Elastomer and Tyre Research Institute, Rajasthan, India. Methanol and chloroform (RANKEM, India) were used as received.

Synthesis of natural rubber–magnetite nanocomposites (NR–MN)

Magnetite nanoparticles (12 ± 5 nm by TEM) were synthesized as reported earlier.[15] The NR–MN nanocomposites were prepared by a solvent casting method. Initially 2 g of dry NR was dissolved in 25 ml of chloroform. The magnetite nanoparticles, synthesized previously, were dispersed in chloroform and sonicated for about 30 min. Then the two solutions were mixed and stirred for 24 h to get a nice blend. The weight ratio of NR to magnetite was 5 : 1. The stirred solution was then added to methanol under vigorous stirring. The black rubbery coagulum (NR–MN) was then filtered, compressed to sheets and dried under vacuum at room temperature.

Synthesis of epoxidized natural rubber (ENR)

5 g of dry natural rubber was dissolved in 50 ml of chloroform in a round bottom flask. Under continuous stirring, the dissolved rubber was acidified by adding 3 ml of formic acid. The temperature of the reaction was lowered to 0 °C using an ice bath. Then, 7 ml of hydrogen peroxide was added dropwise over 30 min. The reaction mixture was stirred for 2 h, while maintaining the temperature at 0 °C. The reaction mixture was then poured into methanol to obtain epoxidized natural rubber (ENR-2 h); 2 h represents the time of epoxidation reaction. Methanol was found to be the best solvent for precipitation as it provided a better yield. The precipitated ENR was filtered and pressed to thin sheets and the sheets were dried under vacuum at 50 °C. The same experimental procedure was repeated for a higher reaction period (6 h) to get ENR of a higher degree of epoxidation (ENR-6 h). All the epoxidized samples were denoted by suffixing them with the reaction periods appropriately.

Synthesis of epoxidized natural rubber–magnetite nanocomposites (ENR–MN)

5 g of NR was dissolved in 50 ml of chloroform in a 250 ml round bottom flask. The magnetite nanoparticles were dispersed in chloroform and sonicated for about 30 min. Then the two solutions were mixed and stirred for 24 h. The weight ratio of rubber to magnetite was 5 : 1. Then the epoxidation reaction was carried out as specified in the previous paragraph. The nanocomposite obtained was made into sheets by compression, dried under vacuum at room temperature and

labeled as ENR–MN-2 h. The same experimental procedure was repeated with a higher reaction period (6 h) for obtaining ENR–MN with a higher degree of epoxidation (labeled as ENR–MN-6 h). Because of the tack of the rubber, unnecessary exposure to the atmosphere was avoided.

Oil absorption studies

Absorption efficacy of all the absorbents was determined by the gravimetric method. All the absorption tests were performed at 25 ± 3 °C. Initially, the absorbents (3 cm × 3 cm) were weighed accurately, using a digital balance of the resolution of 0.1 mg. The weighed sorbents were then submerged in gasoline floating on the surface of water. The sorbents were then taken out of the oil layer using tweezers and hung in the air until all the surface oil drops could be removed through dripping. To monitor the mass of the absorbent as a function of time, the absorbent was removed from the oil at selected intervals, for weighing. All the experiments were duplicated.

The percentage absorption of oil was calculated using the equation

$$\text{Percentage absorption} = \{(W_t - W_0)/W_0\} \times 100$$

where W_0 = weight of the dry absorbent before immersion and W_t = weight of the absorbent after time 't'.

Recovery of the absorbents

Magnetically active absorbents *viz.* NR–MN and ENR–MN in the form of small sheets were directly removed from the oil surface using an NdFeB magnet. This procedure could be applied in the field by opting for larger sheets and powerful magnets. All the other absorbents that were magnetically non-active were pulled out using tweezers, after the absorption.

Effect of water on the sorption efficiency

As the sorbents have to be used to recover the spilled oil in the presence of water, the dampening effect of the absorbents by water was tested. The absorbents were immersed and completely soaked in fresh water. Then they were hung in the air to allow loosely bound water to drip from the sorbent sheets for 30 s. The gain in the mass was noted down before carrying out the oil absorption experiments.

Influence of temperature on the sorption efficiency

A series of experiments were performed to assess the effect of temperature on the oil sorption efficiency by measuring the percentage absorption after 1 h, at different temperatures *viz.* 0 °C, 10 °C, 25 °C and 40 °C. NR, ENR-2 h, ENR-6 h, NR–MN and ENR–MN were used for this study.

Characterizations

The TEM image of the synthesized magnetite nanoparticles was taken using a Philips CM12 transmission electron microscope. The sample was prepared by the deposition and drying of a drop of the nanoparticles dispersed in ethanol onto a formvar coated 400 mesh copper grid before acquiring the micrographs. Scanning electron microscopic analysis was done with a FEI Quanta200 scanning electron microscope. Magnetite nanoparticles were used as such whereas all the other samples were analyzed as films by drop casting a thin film on a silicon wafer followed by vacuum drying. The films were sputter coated with carbon prior to the analysis. The operating voltage was maintained at 30 kV. Thermogravimetric studies were carried out with a Perkin Elmer TGA-7 thermogravimetric analyzer. The samples were heated at 20 °C min^{-1} under a flowing N_2 atmosphere. Differential scanning calorimetry measurements were made using a TA Instruments Q200 modulated differential scanning calorimeter equipped with a liquid nitrogen sub-ambient cooling accessory and employing nitrogen as the flow gas. All the samples were encapsulated in standard aluminium pans. The samples were pretreated at 100 °C for about 5 min, quenched rapidly to −90 °C, *i.e.*, below the anticipated glass transition temperature (T_g), and scanned upwards at 10 °C min^{-1}. All the heating and cooling cycles were repeated to ensure precise T_g values. X-ray diffraction patterns of all the materials were recorded with a Bruker D8 Advance diffractometer equipped with a Cu anode and a Cu Kα source of the wavelength of 1.5406 Å. MNs were analyzed in the powder form whereas all the other samples were analyzed as fine films coated on the powder XRD glass plates. The crystallite size of magnetite was calculated by applying the Scherrer formula for each peak and then their mean value was assessed. ^{1}H NMR spectra were obtained using a Bruker AV 400 (400 MHz) spectrometer. Samples of the concentration of 3% w/v in $CDCl_3$ were used for the analysis. Tetramethylsilane (TMS) was used as the internal standard.

Results and discussion

Prior to the synthesis of ENR–MN nanocomposites, MNs were synthesized *via* a coprecipitation method. The mean diameter of the synthesized MNs is calculated to be 12 ± 5 nm (Fig. 1) from the TEM image of the nanoparticles. The X-ray diffraction data of MNs (Fig. 5) confirmed the presence of pristine magnetite and the average size of MNs was found to be 22 ± 3 nm. The diffraction peaks observed at 2θ = 30.12°, 35.48°, 43.12°, 57.02° and 62.62° correspond to (2 2 0), (3 1 1), (4 0 0),

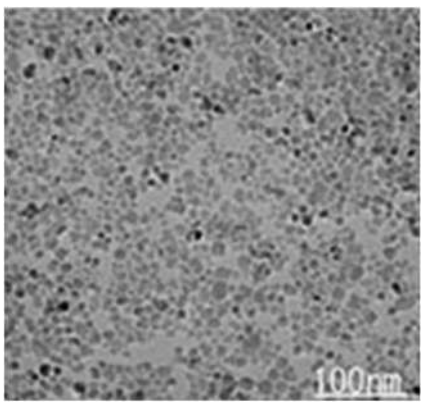

Fig. 1 TEM image of the MNs.

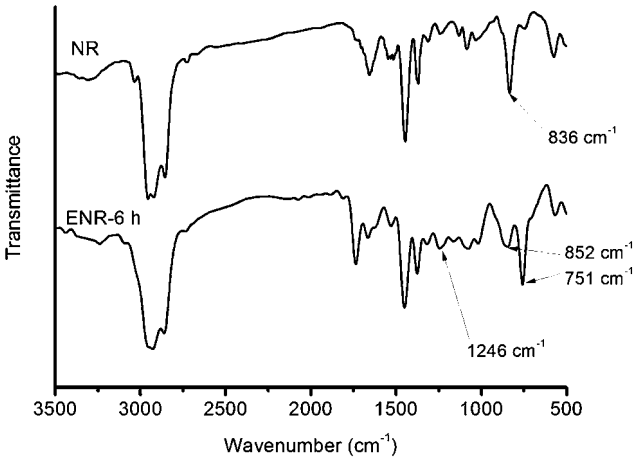

Fig. 2 FTIR spectra of NR (above) and ENR-6 h (below).

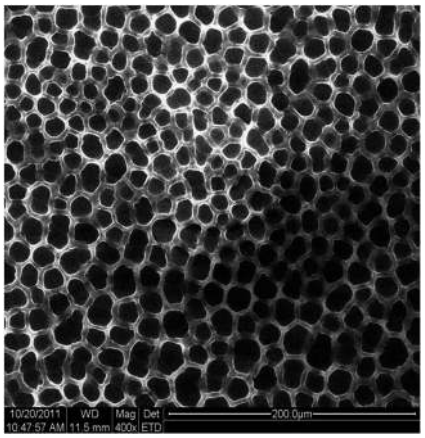

Fig. 3 SEM image of ENR-6 h.

(4 4 0) and (5 1 1) planes of magnetite, respectively (ICDD card no.88-0866). The elemental analysis of the MNs as determined by energy dispersive X-ray studies (Fig. S1†) revealed the weight percentage of iron and oxygen to be 71.98 and 28.02, respectively, thus confirming the presence of pure magnetite.

ENRs with two different degrees of epoxidation were prepared as detailed in the Experimental section earlier. The FT-IR spectrum of the ENR (Fig. 2) indicated the presence of the oxirane ring, as evident from the intense peaks at 751 cm^{-1}, 852 cm^{-1} and 1246 cm^{-1} which could be assigned to the symmetric and asymmetric stretching vibrations of the C–O–C bond, confirming the formation of epoxides. The IR spectrum of NR showed a strong signal at 836 cm^{-1} arising due to the double bond and all the other peaks mentioned above were absent. The NMR spectrum of ENR showed a new peak at 2.7 ppm due to the methine proton attached to the oxirane ring, in contrast to that of NR. The signal due to the olefinic protons (5.1 ppm) was found to diminish in intensity with the extent of epoxidation reaction. The percentage epoxidation was calculated from the intensities of the methine signal at 2.7 ppm and the olefinic proton signal at 5.1 ppm, as reported earlier.[16] The extents of epoxidation were estimated to be 5 mol% for the reaction period of 2 h and 37.5 mol% for the reaction period of 6 h (Fig. S2†). The ENR–MN nanocomposites could not be analyzed by NMR owing to the presence of superparamagnetic magnetite nanoparticles.

The glass transition temperature (T_g) of the ENR was determined by differential scanning calorimetry (DSC). The T_g of natural rubber was −68 °C and with epoxidation time, the T_g was found to increase (Table 1) as reported earlier, which suggests that the T_g of natural rubber increases by 0.92 °C for every mol% epoxidation.[17] The greater T_g is attributed to the presence of a compact network structure in ENR. The degrees of epoxidation were calculated from the variation in T_g values and were found to be 6 mol% and 35 mol% for the reaction periods of 2 h and 6 h, respectively (5 mol% and 37.5 mol% respectively from NMR spectra). The DSC curve for ENR showed a strong, exothermic peak, in the temperature range of 260 to 320 °C, which could be attributed to the ring opening of the epoxy rings at elevated temperatures.[18]

ENR forms "breath figures" when cast onto a silicon wafer surface from solution, under very high humidity conditions as observed under SEM (Fig. 3). The formation of "breath figures" and the mechanism of the same have been discussed widely in the literature.[19]

ENR–MNs were synthesized by carrying out the epoxidation reaction in the presence of magnetite nanoparticles for the first time. The percentage epoxidation of ENR (performed in the presence of MNs) could not be resolved by the analytical

Table 1 T_g values of all the absorbents

Samples	T_g (in °C) at the heating rate of 10 °C min^{-1}
NR	−68.0
NR–MN	−65.3
ENR-2 h	−62.4
ENR–MN-2 h	−13.1
ENR-6 h	−35.6
ENR–MN-6 h	−5.4

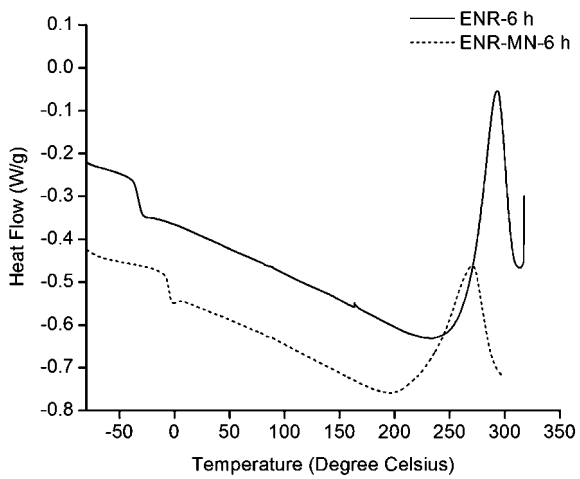

Fig. 4 DSC curves of ENR-6 h and ENR–MN-6 h (heating rate 10 °C min^{-1}).

methods employed. NMR spectroscopy and DSC technique were not useful to determine the extent of epoxidation due to the presence of MNs. The nanocomposite films coated on the CsCl crystals were extremely opaque due to the presence of magnetite nanoparticles, which resulted in poor spectral quality. The DSC data for the ENR–MN nanocomposite provided evidence for the presence of epoxide rings in the nanocomposite. A strong exothermic peak arising out of the ring opening confirmed successful epoxidation reaction in the presence of MNs. Here the ring opening is initiated at a relatively lower temperature in the case of ENR–MN in comparison to ENR. This suggested that MNs act as a Lewis acid catalyst[20] and assist in the ring opening. The DSC of ENR–MN-6 h suggested that the inclusion of crystalline iron oxide nanoparticles changed the T_g of ENR-6 h drastically from −36 °C to −5 °C (Fig. 4). This could be due to the magnetite (moisture induced) activated ring opening of the oxirane rings.[21] This eventually would increase the degree of crosslinking and in turn the immobility of molecules. As a result, a remarkable change in the T_g of ENR occurred. However, the magnitude of increase in T_g for NR–MN was relatively less, indicating that the NR did not interact strongly with the MNs while ENR did (Fig. S3†).

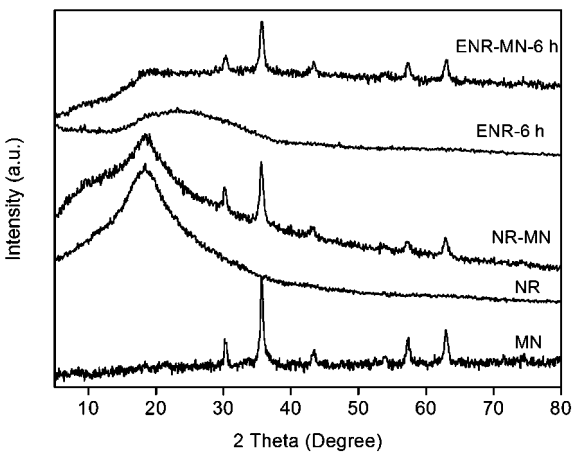

Fig. 5 X-ray diffraction spectra of the MN, NR, ENR-6 h and the nanocomposites.

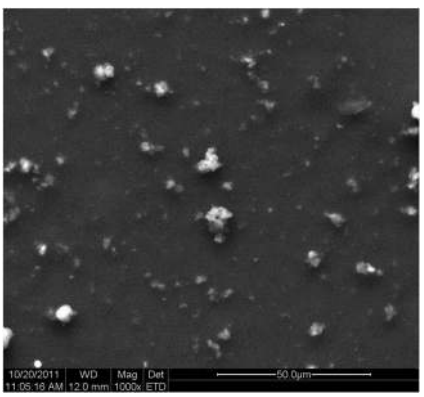

Fig. 6 SEM image of ENR–MN-6 h.

The XRD patterns of NR–MN and ENR–MN-6 h (Fig. 5) suggest that the nanocomposites consist of amorphous regions that appear as a halo at around $2\theta = 20°$ and typical narrow diffraction peaks arise out of the crystalline phase consisting of magnetite nanoparticles. The insertion and the subsequent migration of crystalline magnetite into the rubber matrix decreased the total amorphous domains of the original rubber.[22] The SEM image (Fig. 6) of the ENR–MN nanocomposite reveals that the MN is present by and large as nanoparticles with the diameter of the order of ~30 nm with some agglomerated particles with size ranging from ~100 to ~900 nm.

TGA of NR–MN and ENR–MN nanocomposites (Fig. S4†) enables the precise estimation of the weight percentage of MN present in the composite. All the TGA curves implied a single step degradation mechanism for all the samples and the residual sample remaining at the end directly gave the amount of magnetite nanoparticles loaded in NR–MN and ENR–MN-6 h, which were 10 and 20 weight%, respectively. Although 20 weight % of MN was initially mixed with NR in chloroform, the actual weight percentage of MN in the NR–MN nanocomposite was found to be 10%. This is due to poor miscibility of MN in NR. However, in the case of ENR–MN all the MNs that were added are present in the nanocomposite suggesting that MN mixes well with ENR. From the TGA results, it was observed that the temperature at which 10% weight degradation ($T_{10\%}$) occurs had been enhanced substantially in the case of magnetite coated rubbers. $T_{10\%}$ values for NR, NR–MN, ENR and ENR–MN-6 h were 282 °C, 375 °C, 349 °C and 388 °C, respectively. Earlier reports also proposed improvement in thermal stability of the natural rubber nanocomposite[23a] and the silicone polymer nanocomposite[23b] with the addition of iron oxide.

Absorption of petrol (gasoline)

Natural rubber is notorious for low oil resistance due to its high solubility in oil. This oil absorbing nature of natural rubber, which is normally considered as a shortcoming, is exploited here for potential oil spill treatment. The oil absorbing property of natural rubber decreases significantly with the extent of epoxidation as the solubility in oil decreases.[24] ENR-2 h and ENR-6 h were used as oil absorbents since they were also elastomers, similar to unepoxidized natural rubber, and in addition they bind MN very well thus enabling post-oil absorption recovery by the application of a magnetic field. It may be noted that ENRs with higher degrees of epoxidation produce a material, which is not rubbery and therefore, ENR with greater than

Table 2 Oil absorption data for all the absorbents

Absorbent	Percentage absorption after 1 h	Maximum absorption (g of oil per g of absorbent)
NR	290	38.5 (after 15 h)
NR–MN	215	6.5 (after 5 h)
ENR-2 h	230	25.6 (after 24 h)
ENR–MN-2 h	118	2.6 (after 2 h)
ENR-6 h	195	9.7 (after 24 h)
ENR–MN-6 h	100	6.8 (after 15 h)

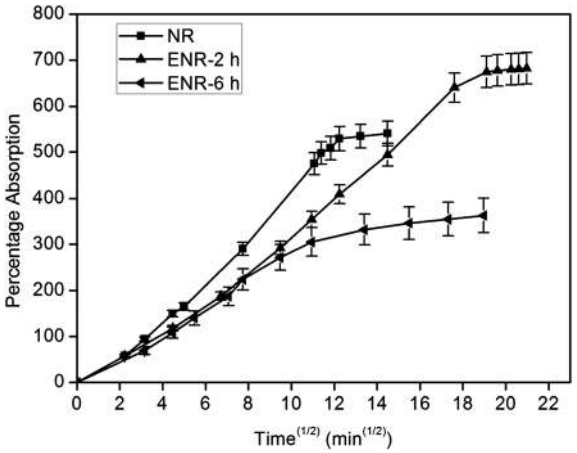

Fig. 7 Percentage absorption (% w/w) of petrol *vs.* time$^{(1/2)}$ for NR, ENR-2 h and ENR-6 h.

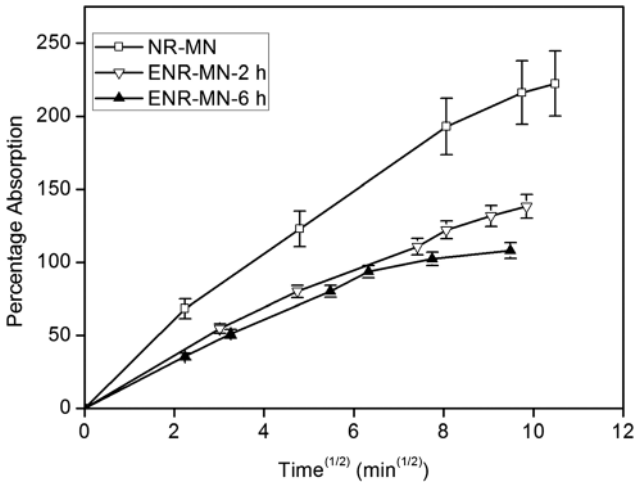

Fig. 8 Percentage absorption (% w/w) of petrol *vs.* time$^{(1/2)}$ for NR–MN, ENR–MN-2 h and ENR–MN-6 h.

40 mol% of epoxidation is not suitable for oil absorption studies as the recovery of the oil may not be possible by squeezing or by any other mechanical treatments.

In the oil absorption studies reported here, petrol was used as a substituent for crude oil due to its ready availability and the results obtained thus are likely to reflect the results that would be obtained with crude oil. Petrol absorption studies were conducted as reported elsewhere.[7] The oil absorption efficiency of unmodified NR was assessed and used as a model. NR was found to absorb oil quicker than all the other sorbents as expected (Table 2 and Fig. 7). 1 g of NR absorbed up to ~39 g of petrol while ~0.2 g is lost due to dissolution. Beyond this point, NR completely got saturated. The dissolution of NR increased linearly with its exposure time to petrol. In the case of epoxidized analogues, ENR-2 h absorbed slightly less amount of petrol and the process was slower in comparison with the unmodified NR. The presence of the cross-linked gel phase in ENR reduces the diffusivity of petrol into the polymer matrix. The reduction in the quantity and rate of oil absorption could be additionally rationalized by the increase in polarity accompanying epoxidation. The maximum petrol absorption capacity of ENR-2 h was 26 g per g after 24 h. In the case of ENR-6 h, both the rate and amount of oil absorbed were fairly low because of the relatively higher epoxide content. Consequently, 1 g of ENR-6 h absorbed up to ~10 g of petrol in 24 h. No mass loss was observed even after three days of immersion. The ENR-6 h absorbs petrol very slowly. When the petrol absorption capabilities of ENR with two different extents of epoxidation are compared, it is noted that the ENR with a higher extent of epoxidation being less hydrophobic absorbs less quantity of petrol (Table 2 and Fig. 7).

The petrol absorption kinetic studies of the NR–MN nanocomposite revealed that the maximum petrol uptake was ~6.5 g per g after 5 h. The maximum petrol uptake capacities of ENR–MN-2 h and ENR–MN-6 h were 2.6 and 6.8 g per g, respectively (Table 2). While comparing the petrol absorption of ENR–MN and NR–MN, it could be observed that NR–MN absorbed petrol relatively faster than ENR–MN. Though the maximum absorption for NR–MN could be more than this, the saturation value could not be found out as the nanocomposite started mixing with petrol after 5 h. ENR–MN-2 h was found to dissolve after 5 h of immersion in petrol whereas ENR–MN-6 h was very stable in petrol even after 24 h of immersion. The corresponding kinetic data for ENR without magnetite indicate that the absorption of petrol in unfilled ENR is much faster as there are no obstacles for the diffusion/permeation process. The petrol absorption kinetic data for the nanocomposites are shown in Fig. 8.

The photographic image of the ENR–MN-6 h nanocomposite, with absorbed oil, in the presence of a rare earth magnet is shown in Fig. 9a. The effect of water on oil absorption was also studied and this showed negligible extent of water absorption (0.01%) by the materials used. The materials used were lighter than water and are seen to float on the water surface as shown by an example in Fig. 9b. In this picture the bottom layer is aqueous copper sulphate solution and the top layer is petrol where the ENR–MN floats exactly on the top of the aqueous layer.

To benchmark the results from these studies the following additional experiments were conducted. Butyl rubber (BR), the

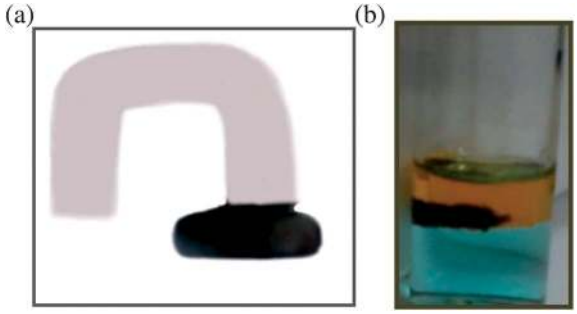

Fig. 9 (a) ENR–MN, post-petrol absorption attracted by a magnet; (b) ENR–MN, post-petrol absorption floating at the petrol–water interface as contrasted by the addition of $CuSO_4$ to the aqueous layer.

most commonly used rubber for oil spill recovery, was also tested for its sorption capability and was found to lose its hardness after 2 h of immersion in petrol. The amount of oil uptake was ~1 g per g, which was very less when compared to the other sorbents studied in this work. Butyl rubber mixed completely with petrol within 3 h forming a very high viscous gel and hence was not amenable to simple oil absorption studies. The petrol absorption rates of NR, NR–MN and BR were much higher than those of epoxidized analogues, as expected. The absorption of oil using various eco-friendly materials has been reported. Choi and Cloud reported that cotton, milkweed and kapok have an oil absorption capacity of 30–40 g per g, which is the highest oil absorption capacity known so far.[3] But these materials also have a higher uptake of water which is not encouraging during oil recovery. Similar reports are available for oil sorptions that make use of common materials, with slight modification in their structure. Some of the important modified sorbents with higher oil absorption are acylated rice straw with an absorption capacity of 16–24 g per g, cross-linked butyl rubber with an absorption capacity of 15–23 g per g and acylated cellulose with an absorption capacity of 20 g per g.[25a,25b,4d] These modifications increase the stability and hydrophobicity and subsequently enhance selective affinity towards oil.

Reusability studies and the effect of temperature

The reusability studies were carried out only for the absorbents that remained undissolved even after saturation. NR, NR–MN and ENR–MN-2 h were found to lose mass upon and during the oil absorption process. Therefore ENR-2 h, ENR-6 h and ENR–MN-6 h alone were investigated for recyclability. All the absorbents were squeezed with the help of tissue paper and were dried at 50 °C. The reusability experiments indicate that the maximum oil absorption of ENR-2 h, ENR-6 h and ENR–MN-6 h decreases with an increase in the number of cycles. The maximum petrol absorption values (g of oil per g of absorbent) of ENR-2 h, ENR-6 h and ENR–MN-6 h have been plotted against the number of cycles (up to 5 cycles) in Fig. 10. It may be noted

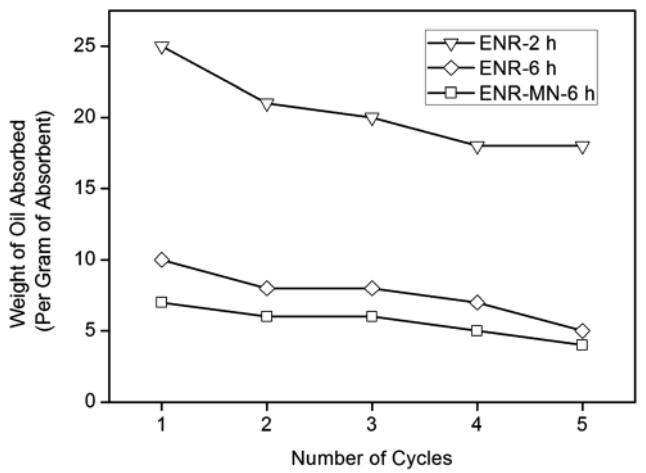

Fig. 10 Recyclability plots for ENR-2 h, ENR-6 h and ENR–MN-6 h.

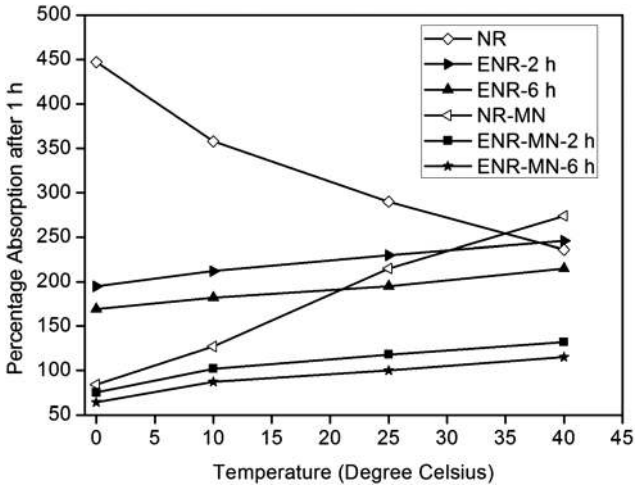

Fig. 11 Effect of temperature *versus* % petrol absorption plots for all the absorbents.

that no other specific activation was required before carrying on the next cycle.

The impact of temperature on the oil absorption was also studied at four different temperatures. The percentage absorption values after 1 h are plotted against temperature and presented in Fig. 11 for all the absorbents. The petrol absorption efficacies of all the absorbents except NR decreased with the decrease in the temperature from 40 °C to 0 °C. Johnson and Thomas reported that the maximum hexane uptake decreased for NR and increased for ENR with the increase in temperature.[26] The presence of the highly cross-linked gel phase in ENR and the other nanocomposites could be attributed for this temperature dependence in comparison to NR. When the temperature was reduced to 0 °C, the chain flexibility in ENR was reduced relative to that at 40 °C to allow the oil to enter into its matrix. At temperatures higher than 40 °C, it was expected to absorb more as a result of more flexibility. Therefore the rate of diffusion as well as the maximum oil uptake in ENR was directly proportional to temperature. In the case of NR–MN and ENR–MN, the oil uptake ability decreased with the decrease in temperature. These highly cross-linked nanocomposites were too rigid at lower temperatures to allow the oil to diffuse inside them.

Influence of porosity on oil absorption

In the light of the results obtained and based on the principles of capillary action that pores in the absorbing material could enhance oil absorption, the effect of porosity in the rubber matrix on the oil absorption was investigated. Porous ENR was synthesized by using silica nanoparticles filled NR in epoxidation followed by the removal of silica using HF dissolution. The synthetic procedure and characterization are given in the ESI.† Even though porous ENR absorbed petrol better than all the other absorbents, it could not reach the absorption rate of NR. This might be due to the presence of a negligible amount of unremoved silica (white fraction in Fig. S5†) that could act as a

hindrance to the oil. However the complete removal of silica nanoparticles enhanced absorption and ~19 g of petrol was absorbed by one gram of the porous ENR absorbent. This absorbent was found to retain its structural integrity in petrol for many weeks. The absorption capacity of porous ENR thus synthesized is greater than that of nonwoven polypropylene, a widely used commercial absorbent.

Conclusion

Mild epoxidation of natural rubber, in the presence of magnetite, results in a petrol absorbing composite that is magnetically recoverable. The extent of epoxidation is controlled in such a manner that the NR does not lose its elasticity while retaining its ability to absorb oil while binding to sufficient quantity of MNs for magnetic recovery. ENR with 5 mol% of epoxidation served as the best absorbent among all the absorbents and it was stable in petrol even after many days of immersion. In the case of the ENR–MN-6 h nanocomposite, the absorption of petrol was found to be less and slower. Even though the maximum oil uptake was less (~7 g per g) for ENR–MN-6 h, no mass loss was observed even after immersion in petrol for many weeks. Hence the material could be reused for several cycles without much loss in the capacity. In addition to being eco-friendly, ENR–MN-6 h has comparatively greater petrol uptake than that of butyl rubber, which is the most commercially used rubber. Porous ENR was also synthesized for the first time. Porous ENR absorbed a relatively larger amount of petrol and exhibited the highest stability in petrol. The sorbents used have quite high absorption capacities to be applied practically with very low water uptake and a few of the absorbents could be satisfactorily reused. Thus new, eco-friendly nanocomposite materials have been synthesized from natural rubber, for the first time, for the removal of oil spills.

References

1 L. Guterman, *Science*, 2009, **323**, 1558–1559.
2 B. E. Ornitz and M. A. Champ, *Oil Spills First Principles: Prevention and Best Response*, Elsevier Science Ltd., Oxford, U.K., 2002.
3 H. M. Choi and R. M. Cloud, *Environ. Sci. Technol.*, 1992, **26**, 772–776.
4 (*a*) E. Witka-Jezewska, J. Hupka and P. Pieniazek, *Spill Sci. Technol. Bull.*, 2003, **8**, 561–564; (*b*) T. R. Annunciado, T. H. D. Sydenstricker and S. C. Amico, *Mar. Pollut. Bull.*, 2005, **50**, 1340–1346; (*c*) S. S. Banerjee, M. V. Joshi and R. V. Jayaram, *Chemosphere*, 2006, **64**, 1026–1031; (*d*) G. Deschamps, H. Caruel, M. E. Borredon, C. Bonnin and C. Vignoles, *Environ. Sci. Technol.*, 2003, **37**, 1013–1015; (*e*) M. M. Radetic, D. M. Jocic, P. M. Jovancic, Z. L. J. Petrovic and H. Thomas, *Environ. Sci. Technol.*, 2003, **37**, 1008–1012; (*f*) M. Hussein, A. A. Amer and I. I. Sawsan, *Int. J. Environ. Sci. Technol.*, 2008, **5**, 233–242; (*g*) J. T. Korhonen, M. Kettunen, R. H. A. Ras and O. Ikkala, *ACS Appl. Mater. Interfaces*, 2011, **3**, 1813–1816.
5 (*a*) E. L. Schrader, A Practical Composition of Organic, Synthetic and Inorganic Sorbents, *Clean Gulf 93 and the American Chemical Society Conference, Emerging Technology in Hazardous Waste Management*, 1993, pp. 17–22; (*b*) J. S. Yang, M. N. Cho, B. K. Kim and M. Narkis, *J. Appl. Polym. Sci.*, 2005, **98**, 2080–2087; (*c*) S. Bhattacharya and Y. Krishnan-Ghosh, *Chem. Commun.*, 2001, 185–186; (*d*) S. Basak, J. Nanda and A. Banerjee, *J. Mater. Chem.*, 2012, **22**, 11658–11664.
6 (*a*) O. K. Karakasi and A. Moutsatsou, *Fuel*, 2010, **89**, 3966–3970; (*b*) J. G. Reynolds, P. R. Coronado and L. W. Hrubesh, *J. Non-Cryst. Solids*, 2001, **292**, 127–137; (*c*) M. Toyoda, J. Aizawa and M. Inagaki, *Desalination*, 1998, **115**, 199–201; (*d*) M. O. Adebajo, R. L. Frost, J. T. Kloprogge, O. Carmody and S. Kokot, *J. Porous Mater.*, 2003, **10**, 159–170; (*e*) M. Roulia, K. Chassapis, Ch. Fotinopoulos, Th. Savvidis and D. Katakis, *Spill Sci. Technol. Bull.*, 2003, **8**, 425–431.
7 Q. F. Wei, R. R. Mather, A. F. Fotheringham and R. D. Yang, *Mar. Pollut. Bull.*, 2003, **46**, 780–783.
8 J. H. Bradbury and M. C. S. Perera, *Ind. Eng. Chem. Res.*, 1988, **27**, 2196–2203.
9 J. E. Davey and J. R. Loadman, *Br. Polym. J.*, 1984, **16**, 134–138.
10 A. S. Hashim and S. Kohjiya, *J. Polym. Sci., Part A: Polym. Chem.*, 1994, **32**, 1149–1157.
11 I. R. Gelling, *NR Technol.*, 1987, **18**, 21–29.
12 R. M. Cornell and U. Schwertmann, *The Iron Oxides: Structure, Properties, Reactions, Occurrences and Uses*, Wiley-VCH, Weinheim, 2nd edn, 2003.
13 (*a*) S. Mornet, S. Vasseur, F. Grasset and E. Duguet, *J. Mater. Chem.*, 2004, **14**, 2161–2175; (*b*) J. Wan, W. Cai, X. Meng and E. Liu, *Chem. Commun.*, 2007, 5004–5006; (*c*) S. Sun, C. B. Murray, D. Weller, L. Folks and A. Moser, *Science*, 2000, **287**, 1989–1992; (*d*) T. S. Anirudhan and S. Sandeep, *J. Mater. Chem.*, 2012, **22**, 12888–12899; (*e*) J. H. Jung, J. H. Lee and S. Shinkai, *Chem. Soc. Rev.*, 2011, **40**, 4464–4474.
14 J. E. Turbeville, *Environ. Sci. Technol.*, 1973, **7**, 433–438.
15 K. Babu and R. Dhamodharan, *Nanoscale Res. Lett.*, 2008, **3**, 109–117.
16 T. Saito, W. Klinklai and S. Kawahara, *Polymer*, 2007, **48**, 750–757.
17 *Natural Rubber Science and Technology*, ed. D. Roberts, Oxford University Press, Oxford, U.K., 1990.
18 A. T. Riga and L. Judovits, *Materials Characterization by Dynamic and Modulated Thermal Analytical Techniques*, ASTM STP 1402, Library of Congress Cataloguing-in-Publication Data, 2001.
19 A. V. Vivek, K. Babu and R. Dhamodharan, *Macromolecules*, 2009, **42**, 2300–2303.
20 W. Weiss and R. SchlÖgl, *Top. Catal.*, 2000, **13**, 75–90.
21 N. Sharma, M. S. Kumar and B. C. Ray, *J. Reinf. Plast. Compos.*, 2007, **26**, 1083–1089.
22 D. Puryanti, S. H. Ahmad, M. H. Abdullah and A. N. H. Yusoff, *Int. J. Polym. Mater.*, 2007, **56**, 1–12.

23 (*a*) H. Ismail, S. T. Sam, A. F. Mohd Noor and A. A. Bakar, *Polym.-Plast. Technol. Eng.*, 2007, **46**, 641–650; (*b*) L. G. Hanu, G. P. Simon and Y. B. Cheng, *Polym. Degrad. Stab.*, 2006, **91**, 1373–1379.
24 V. Tanrattanakul, B. Wattanathai, A. Tiangjunya and M. Putsadee, *J. Appl. Polym. Sci.*, 2003, **90**, 261–269.
25 (*a*) X. F. Sun, R. Sun and J. X. Sun, *J. Agric. Food Chem.*, 2002, **50**, 6428–6433; (*b*) D. Ceylan, S. Dogu, B. Karacik, S. D. Yakan, O. S. Okay and O. Okay, *Environ. Sci. Technol.*, 2009, **43**, 3846–3852.
26 T. Johnson and S. Thomas, *Polymer*, 2000, **41**, 7511–7522.